EUROPEAN JOURNAL OF PURE AND APPLIED MATHEMATICS
2026, Vol. 19, Issue 2, Article Number 6800
ISSN 1307-5543 – ejpam.com
Published by New York Business Global

A Computational Study of the Fractal–Fractional Benney Equation Using the Laplace–Adomian Method and Neural Network Validation

Sadique Ahmad[1], Israr Ahmad[2], Zeeshan Ali[3,*], Fady Hasan[4], Nabil Mlaiki[4]

[1] *EIAS Data Science and BlockChain Laboratory, College of Computer and Information Sciences,Prince Sultan University,Riyadh 11586, Saudi Arabia*
[2] *Department of Mathematics, Government Post Graduate Jahanzeb College, Swat, Khyber Pakhtunkhwa, Pakistan*
[3] *Department of Information Management, National Yunlin University of Science and Technology, Douliu, Yunlin, Taiwan, R.O.C*
[4] *Department of Mathematics and Sciences, Prince Sultan University Riyadh, 11586, Saudi Arabia*

Abstract. In this research, the nonlinear Benney equation (BE) is examined in a fractal-fractional (FF) context with a power-law derivative. Qualitative and quantitative approaches are investigated. To study the qualitative aspects, the theory of functional analysis is used, and the Laplace Adomian decomposition method (LADM) is used to obtain an approximate analytical solution. The validity of the method is demonstrated in two numerical examples. The robustness and accuracy of the results obtained with LADM are further checked by employing a neural network (NN) approach with the Levenberg–Marquardt (LM) algorithm, complemented by regression statistics and error distribution. The suggested hybrid approach shows an outstanding correlation between analytic and predicted solutions and brings forth the effect of fractional and fractal parameters on the transmission of nonlinear dispersive waves. The research advances hybrid mathematical and computational methods for modelling memory-dependent and self-similar processes and has potential applications in fluid dynamics, nonlinear optics, and the investigation of complex systems.

2020 Mathematics Subject Classifications: 26A33, 34A08, 03C65.

Key Words and Phrases: Fractal-Fractional, qualitative analysis, laplace transform, series solution, neural network validation.

*Corresponding Author.
DOI: https://doi.org/10.29020/nybg.ejpam.v19i2.6800

Email addresses: `saahmad@psu.edu.sa` (S.Ahmad), `israrahmadjc503@gmail.com` (I.Ahmad) `zeeshanalinsr@gmail.com` (Z.Ali), (fhasan@psu.edu.sa) (F.Hasan), `nmlaiki@psu.edu.sa` (N.Mlaiki)

1. Introduction

Fractional calculus, whose origins date back to the correspondence between Leibniz and L'Hôpital, has evolved into a fundamental mathematical tool for modelling complex phenomena. The successive contributions of eminent mathematicians such as Fourier, Grünwald, Letnikov, and Hadamard [1–3] have progressively enriched this field, leading to the fundamental definitions of Riemann–Liouville and Caputo [4, 5], which today constitute the theoretical foundations of modern fractional calculus.

The emergence of fractional operators has been structured around two major families characterized by the nature of their kernels. On one hand, there are operators with singular kernels, typically of the power-law type; on the other hand, operators with non-singular kernels, involving exponential or Mittag–Leffler functions [6–10]. This diversification has greatly broadened the base of fractional calculus, which is now applied in various fields such as biology, chemistry, signal processing, control theory, and physical modelling [11–14].

The more recent incorporation of fractal ideas into the fractional framework gave rise to the concept of fractal–fractional derivatives (FFDs), a huge conceptual leap. These hybrid operators utilize mathematically advanced kernels like the power-law, Mittag–Leffler function, and generalized exponential decay [15, 16]. The power of FFDs is that they can capture two intrinsic properties of complex systems concurrently: memory effects through the fractional order parameter θ, and self-similarity features through the fractal dimension parameter κ [17].

The applications of FFDs illustrate their scientific importance and flexibility. Within the biomedical applications area, they have been used to simulate glucose–insulin behaviour through the Atangana–Baleanu derivative [18, 19] to study the spread of diseases like malaria [20] and dengue [21]. Their applications also lie in the study of chaotic attractors [22], the dynamics of ferromagnetic fluids [23], and theoretical studies of some epidemiological models [24, 25].

This research on fractional-order partial differential equations (FOPDEs) follows naturally from these theoretical advances. This rapidly developing field has necessitated the extension and application of traditional differential equation techniques to the unique properties of fractional operators. An important example of the versatility of FOPDEs is in their capacity to describe intricate couplings between long and short waves—a common occurrence in physical systems. Asymptotic analysis indicates that the long-wave component amplitude is much less than that of the short-wave component, which is specifically significant in characterizing long waves in shallow water [26].

In this fertile and multidisciplinary scientific background, the current work seeks to further develop the mathematical treatment of FFDs, construct effective numerical techniques for their application, and push their use into new complicated systems, thus making a contribution to knowledge in this fast-developing field.
The BE in the $1 + 1$ dimension is provided by [27]:

$$v_\ell(y,\ell) + (v^n(y,\ell))_y + v_{yy}(y,\ell) + \omega v_{yyy}(y,\ell) + v_{yyyy}(y,\ell) = 0, \tag{1}$$

Here ω is positive constant and n is positive integer. (1), for n=3, can be expressed as:

$$v_\ell(y,\ell) + 3v^2(y,\ell)v_y(y,\ell) + v_{yy}(y,\ell) + \omega v_{yyy}(y,\ell) + v_{yyyy}(y,\ell) = 0. \tag{2}$$

One of the significant contributions to the fields of non-linear wave theory and fluid mechanics is the equation (2). It gives a platform for understanding complex wave dynamics in a range of mediums [28, 29]. The aim of the equation (2) is to address special system problems such as dispersion and wave interaction. All the basic physical parameters required to accurately predict wave interaction and propagation in non-linear systems are encompassed within its equation [30, 31]. Since the aforementioned equation may more correctly replicate complicated processes, it is a valuable tool in both theoretical study and practical applications, from coastal engineering to optical communications (see [32, 33]).

It is evident from the literature that researchers have not focused more on the numerical analysis of FF problems. Recently Eiman et al. [34] have introduced LADM for FF differential problems and studied a population dynamical model. Inspired by the work of Eiman and her co-authors [34], we consider equation (2) under the FF derivative of power law kernel type as follows:

$$\begin{cases} {}^{FF}D^{\theta,\kappa}(v(y,\ell)) + 3v^2(y,\ell)v_y(y,\ell) + v_{yy}(y,\ell) + \omega v_{yyy}(y,\ell) + v_{yyyy}(y,\ell) = 0, \\ {}^{RL}D^{\theta-1}v(y,0) = v_0 = g(y), \quad \theta,\kappa \in (0,1],\, \ell, y \in [0,T] = J. \end{cases} \tag{3}$$

We applied an integral Laplace transform coupled with the decomposition approach to obtain an estimate solution for the previously described equation (3). We give various examples and their corresponding graphs.

We develop existence and uniqueness criteria for the given general problem.

$$\begin{cases} {}^{FF}D^{\theta,\kappa}_{0,\ell}(v(y,\ell)) = \Psi(v(y,\ell),\ell), \\ {}^{RL}D^{\theta-1}v(y,0) = v_0 = g(y). \end{cases} \tag{4}$$

Where the non-linear function $\Psi \in C(R \times J) \to R$ and $g : J \to R$ is continuous and bounded i.e. $\|g\| \leq m$. We create the Banach space to conduct additional research as $\mathbb{Y} = C[0,T] \times R \to R$, where $0 \leq \ell \leq T < \infty$.

The norm is described as:

$$\|v\| = \max_{y,\,\ell \in J} \big| v(y,\ell) \big|.$$

Definition 1. *[34] With a power-law kernel, the FF derivative of a continuous and differentiable function v on J is given by:*

$${}^{FF}D^{\theta,\kappa}_{0,\ell}(v(y,\ell)) = \begin{cases} \dfrac{1}{\Gamma(m-\theta)} \left(\dfrac{d}{d\ell^\kappa}\right)^m \displaystyle\int_0^\ell (\ell-\phi)^{m-\theta-1} v(y,\phi)d\phi, & m-1<\theta<m, \\ \dfrac{1}{\Gamma(m-\theta)} \left(\dfrac{d}{d\ell}\right)^m \displaystyle\int_0^\ell (\ell-\phi)^{m-\theta-1} \quad v(y,\phi)d\phi, & \kappa = 1, \\ \left(\dfrac{d}{d\ell}\right)^m v(y,\ell), \quad \theta = m,\, \kappa = 1. \end{cases}$$

Particularly, if $\theta \in (0,1)$:

$$^{FF}D^{\theta,\kappa}_{0,\ell}(v(y,\ell)) = \frac{1}{\Gamma(1-\theta)}\left(\frac{d}{d\ell^{\kappa}}\right)\int_0^{\ell}(\ell-\phi)^{\theta-1}v(y,\phi)d\phi.$$

Definition 2. *[34] The FF integral, assuming v is a continuous function on J, is given by:*

$$^{FF}I^{\theta,\kappa}_{0,\ell}(v(y,\ell)) = \frac{\kappa}{\Gamma(\theta)}\int_0^{\ell}\phi^{\kappa-1}(\ell-\phi)^{\theta-1}v(y,\phi)d\phi.$$

Definition 3. *[34] The Laplace transform of $^{RL}D^{\theta}_{0,\ell}v(y,\ell)$ is defined as:*

$$\mathbb{L}[^{RL}D^{\theta}_{0,\ell}v(y,\ell)] = s^{\theta}\mathbb{L}[v(y,\ell)] - s^{\theta-1}\, {}^{RL}D^{\theta-1}v(y,0),\ s \geq 0,\ \theta,\kappa \in (0,1].$$

Theorem 1. *[34] Let $\mathbb{B}$ be a convex, closed, and bounded subset of a Banach space $\mathbb{Y}$, and let $\mathbb{T}:\mathbb{B}\to\mathbb{B}$ be a continuous and compact operator. Then $\mathbb{T}$ has at least one fixed point in $\mathbb{B}$.*

The rest of the paper is broken up into five sections. Section 2 discusses qualitative analysis. In Section 3, the process of derivation is examined. Only the numerical simulations are covered in Section 4, while Section 5 presents the NN validation. Section 6 provides a thorough overview of the entire work.

2. Existence and Uniqueness

Lemma 1. *Using definition 2, the following is the solution to the suggested general problem* (4)*:*

$$v(y,\ell) = g(y) + \frac{\kappa}{\Gamma(\theta)}\int_0^{\ell}(\ell-\phi)^{\theta-1}\phi^{\kappa-1}\Psi(v(y,\phi),\phi)d\phi.$$

The operator $\mathbb{T}$ is considered below in order to accomplish the primary goal:

$$\mathbb{T}v(y,\ell) = g(y) + \frac{\kappa}{\Gamma(\theta)}\int_0^{\ell}(\ell-\phi)^{\theta-1}\phi^{\kappa-1}\Psi(v(y,\phi),\phi)d\phi.$$

For further work, make the following assumptions:

- (A_1) The non-linear function Ψ satisfies the following growth condition:

$$\|\Psi(v)\| \leq a_{\Psi} + c\|v\|,\ \ c \geq 0.$$

- (A_2) There exist a constant L_{Ψ}, such that $v_1, v_2 \in \mathbb{Y}$, we have

$$\|\Psi(v_1) - \Psi(v_2)\| \leq L_{\Psi}\|v_1 - v_2\|.$$

Moreover for Ψ there exist $\Psi(0,\ell) = 0$, hold.

Theorem 2. *Under the assumption* (A_2)*, and if* $\Gamma(\kappa+1)\mathbb{T}^{\theta+\kappa-1}L_\Psi < \Gamma(\theta+\kappa)$*, hold. Then, there exists a unique solution for the suggested general problem* (4)*.*

Proof. Consider $v_1(y,\ell)$, $v_2(y,\ell) \in \mathbb{Y}$, we have

$$\begin{aligned}
\|\mathbb{T}v_1 - \mathbb{T}v_2\| &= \max_{y,\ell\in J}\left|\frac{\kappa}{\Gamma(\theta)}\int_0^\ell (\ell-\phi)^{\theta-1}\phi^{\kappa-1}\Psi(v_1,\phi)d\phi - \frac{\kappa}{\Gamma(\theta)}\int_0^\ell (\ell-\phi)^{\theta-1}\right. \\
&\quad \left.\phi^{\kappa-1}\Psi(v_2,\phi)d\phi\right| \\
&\le \max_{y,\ell\in J}\left\{\frac{\kappa}{\Gamma(\theta)}\int_0^\ell (\ell-\phi)^{\theta-1}\phi^{\kappa-1}|\Psi(v_1,\phi)-\Psi(v_2,\phi)|d\phi\right\} \\
&\le \max_{y,\ell\in J}\left\{\frac{\kappa L_\Psi|v_1-v_2|}{\Gamma(\theta)}\int_0^\ell (\ell-\phi)^{\theta-1}\phi^{\kappa-1}d\phi\right\} \\
&\le \frac{(\kappa+1)T^{\theta+\kappa-1}L_\Psi\|v_1-v_2\|}{\Gamma(\theta+\kappa)}.
\end{aligned}$$

Hence $\mathbb{T}$ has a unique solution.

Theorem 3. *There is at least one solution to the general problem* (4)*, if the assumptions* (A_1, A_2) *are true.*

Proof. To prove that $\mathbb{T}:\mathbb{Y}\to\mathbb{Y}$ full fill the condition of Schaudar fixed point theorem. Suppose closed convex subset $\mathbb{B} = \{v(y,\ell)\in\mathbb{Y} : \|v\| \le r\}$. The proof is divided in the following steps:

Step-1: To show that $\mathbb{T}$ is continuous. Consider a sequence $v_n(y,\ell)$ such that $v_n(y,\ell) \to v(y,\ell)$, we consider

$$\begin{aligned}
\|\mathbb{T}v_n - \mathbb{T}v\| &= \max_{y,\ell\in J}\left|\frac{\kappa}{\Gamma(\theta)}\int_0^\ell (\ell-\phi)^{\theta-1}\phi^{\kappa-1}\Psi(v_n,\phi)d\phi\right. \\
&- \left.\frac{\kappa}{\Gamma(\theta)}\int_0^\ell (\ell-\phi)^{\theta-1}\phi^{\kappa-1}\Psi(v,\phi)d\phi\right| \\
&\le \max_{y,\ell\in J}\frac{\kappa}{\Gamma(\theta)}\int_0^\ell (\ell-\phi)^{\theta-1}\phi^{\kappa-1}\big|\Psi(v_n,\phi)-\Psi(v,\phi)\big|d\phi \\
&\le \frac{\Gamma(\kappa+1)T^{\theta+\kappa-1}L_\Psi\|v_n-v\|}{\Gamma(\theta+\kappa)}.
\end{aligned}$$

Hence $\|\mathbb{T}v_n - \mathbb{T}v\| \to 0$ as $n\to\infty$. Thus $\mathbb{T}$ is continuous.

Step-2: The image of the bounded set under $\mathbb{T}$ is bounded in $\mathbb{Y}$.

$$\begin{aligned}
\|\mathbb{T}v\| &= \max_{y,\ell\in J}\left|g(y) + \frac{\kappa}{\Gamma(\theta)}\int_0^\ell (\ell-\phi)^{\theta-1}\phi^{\kappa-1}\Psi(v,\phi)d\phi\right| \\
&\le \max_{y,\ell\in J}\left\{|g(y)| + \frac{\kappa}{\Gamma(\theta)}\int_0^\ell (\ell-\phi)^{\theta-1}\phi^{\kappa-1}|\Psi(v,\phi)|d\phi\right\}
\end{aligned}$$

$$
\begin{aligned}
&\leq \; m+\frac{\Gamma(\kappa+1)T^{\theta+\kappa-1}(a_{\Psi}+c\|v\|)}{\Gamma(\theta+\kappa)}\\
&\leq \; m+\frac{\Gamma(\kappa+1)T^{\theta+\kappa-1}(a_{\Psi}+cr)}{\Gamma(\theta+\kappa)}.
\end{aligned}
$$

Which shows $\mathbb{T}$ is bounded.
Step-3: To show that $\mathbb{T}$ is equi-continuous, let $\ell_1, \ell_2 \in J$, such that $\ell_1 < \ell_2$.
Consider

$$
\begin{aligned}
\|\mathbb{T}v(y,\ell_1)-\mathbb{T}v(y,\ell_2)\| &= \max_{y,\ell\in J}\Bigg|\frac{\kappa}{\Gamma(\theta)}\int_0^{\ell_1}(\ell_1-\phi)^{\theta-1}\phi^{\kappa-1}\Psi(v,\phi)d\phi\\
&\quad -\frac{\kappa}{\Gamma(\theta)}\int_0^{\ell_2}(\ell_2-\phi)^{\theta-1}\phi^{\kappa-1}\Psi(v,\phi)d\phi\Bigg|\\
&\leq \max_{y,\ell\in J}\Bigg\{\Bigg|\frac{\kappa}{\Gamma(\theta)}\int_0^{\ell_1}(\ell_1-\phi)^{\theta-1}\phi^{\kappa-1}\Psi(v,\phi)d\phi\\
&\quad -\frac{\kappa}{\Gamma(\theta)}\int_0^{\ell_1}(\ell_2-\phi)^{\theta-1}\phi^{\kappa-1}\Psi(v,\phi)d\phi\Bigg|\\
&\quad +\Bigg|\frac{\kappa}{\Gamma(\theta)}\int_{\ell_1}^{\ell_2}(\ell_2-\phi)^{\theta-1}\phi^{\kappa-1}\Psi(v,\phi)d\phi\Bigg|\Bigg\}\\
&\leq (a_{\Psi}+cr)\Bigg\{\frac{\kappa{\ell_1}^{\kappa+\theta-1}B(\theta,\kappa)}{\Gamma(\theta)}\\
&\quad -\frac{\kappa{\ell_1}^{\kappa}{\ell_2}^{\kappa+\theta-2}B\left(\frac{\ell_1}{\ell_2};\kappa,\theta\right)}{\Gamma(\theta)}\\
&\quad +\frac{\kappa{\ell_2}^{\theta+\kappa-1}\left(\Gamma(\kappa)\Gamma(\theta)-B\left(\frac{\ell_1}{\ell_2};\theta,\kappa\right)\Gamma(\kappa+\theta)\right)}{\Gamma(\theta)\Gamma(\kappa+\theta)}\Bigg\}.
\end{aligned}
$$

As $\ell_1 \to \ell_2$ then one can write

$$
B(\frac{\ell_1}{\ell_2};\theta,\kappa)\to B(1;\theta,\kappa)=B(\theta,\kappa)=\frac{\Gamma(\theta)\Gamma(\kappa)}{\Gamma(\theta+\kappa)},
$$

where $B(1;\theta,\kappa)$ is incomplete beta function. After this calculation and as limit $\ell_1 \to \ell_2$, we can write

$$
\|\mathbb{T}v(y,\ell_1)-\mathbb{T}v(y,\ell_2)\|\to 0.
$$

Because of this, $\mathbb{T}$ is equi-continuous and, as a result, meets every requirement of the Schaudar fixed point theorem. It follows that our suggested generic problem (4) has at least one solution since $\mathbb{T}$ has at least one solution.

3. Derivation of the Procedure

Here in this section of the manuscript, we derive the suggested approach. For simplicity some time, we write v instead of $v(y,\ell)$ in our work.

Theorem 4. *The solution of the specified problem* (3) *can be computed as follows under the Laplace transform:*

$$v_0 = g(y),\ v_1 = \mathbb{L}^{-1}\bigg\{\frac{\kappa}{s^\theta}\mathbb{L}\bigg\{-\ell^{\kappa-1}\big(3\mathbb{A}_0 + V_{0yy} + \omega V_{0yyy} + V_{0yyyy}\big)\bigg\}\bigg\},$$

and

$$v_{n+1} = \mathbb{L}^{-1}\bigg\{\frac{\kappa}{s^\theta}\mathbb{L}\bigg[-\ell^{\kappa-1}\big(3\mathbb{A}_n + V_{nyy} + \omega V_{nyyy} + V_{nyyyy}\big)\bigg]\bigg\}, \quad n \geq 0.$$

Proof. As we know that

$$^{FF}D^{\theta,\kappa}(v(y,\ell)) = \kappa^{-1}\ell^{1-\kappa}\, {}^{RL}D^{\theta-1}v(y,\ell)$$

Therfore equation (3), becomes

$$\kappa^{-1}\ell^{1-\kappa}\, {}^{RL}D^{\theta-1}v(y,\ell) + 3v^2v_y + v_{yy} + \omega v_{yyy} + v_{yyyy}. \tag{5}$$

Applying Laplace transform to (5), we have

$$\kappa^{-1}s^\theta V(y,s) - \kappa^{-1}s^{\theta-1}v_0 = \mathbb{L}\big\{-\ell^{\kappa-1}\big(3v^2v_y + v_{yy} + \omega v_{yyy} + v_{yyyy}\big)\big\}. \tag{6}$$

Further, one has from (6)

$$\mathbb{L}\{v(y,\ell)\} = \frac{v_0}{s} + \frac{\kappa}{s^\theta}\mathbb{L}\big\{-\ell^{\kappa-1}\left(3v^2v_y + v_{yy} + \omega v_{yyy} + v_{yyyy}\right)\big\}.$$

Using the initial condition, the preceding equation becomes

$$\mathbb{L}\{v(y,\ell)\} = \frac{g(y)}{s} + \frac{\kappa}{s^\theta}\mathbb{L}\big\{-\ell^{\kappa-1}\big(3v^2v_y + v_{yy} + \omega v_{yyy} + v_{yyyy}\big)\big\}. \tag{7}$$

By applying the inverse transform, we may derive from (7)

$$v(y,\ell) = \mathbb{L}^{-1}\left[\frac{g(y)}{s} + \frac{\kappa}{s^\theta}\mathbb{L}\left\{-\ell^{\kappa-1}\left(3v^2v_y + v_{yy} + \omega v_{yyy} + v_{yyyy}\right)\right\}\right]. \tag{8}$$

The solution is described as:

$$\sum_{n=0}^{\infty} v_n = v,$$

and breaking down the nonlinear terms into

$$\sum_{n=0}^{\infty} \mathbb{A}_n = v^2v_y$$

where $\mathbb{A}_n$ is given by

$$\mathbb{A}_n = \frac{1}{\Gamma(n+1)}\frac{d^n}{d\mu^n}\bigg[\bigg(\Big(\sum_{j=0}^{n}\mu^j v_j\Big)^2\Big(\sum_{j=0}^{n}\mu^j v_j y\Big)\bigg)\bigg]_{\mu=0}.$$

Hence (8) yields

$$\sum_{n=0}^{\infty} v_n(y,\ell) = \mathbb{L}^{-1}\left[\frac{g(y)}{s} + \frac{\kappa}{s^\theta}\mathbb{L}\left\{-\ell^{\kappa-1}\left(3\sum_{j=0}^{n}\mathbb{A}_j + \sum_{j=0}^{n} v_{jyy} + \omega\sum_{j=0}^{n} v_{jyyy} + \sum_{j=0}^{n} v_{jyyyy}\right)\right\}\right].$$

From similar terms on both sides, one can write:

$$v_0 = \mathbb{L}^{-1}\left\{\frac{g(y)}{s}\right\} = g(y), \quad v_1 = \mathbb{L}^{-1}\left\{\frac{\kappa}{s^\theta}\mathbb{L}\left[-\ell^{\kappa-1}\big(3\mathbb{A}_0 + V_{0yy} + \omega V_{0yyy} + V_{0yyyy}\big)\right]\right\}.$$

and so forth. The generic form can be written as:

$$v_{n+1} = \mathbb{L}^{-1}\left\{\frac{\kappa}{s^\theta}\mathbb{L}\left[-\ell^{\kappa-1}\big(3\mathbb{A}_n + V_{nyy} + \omega V_{nyyy} + V_{nyyyy}\big)\right]\right\}, \quad n \geq 0.$$

Remark 1. *The solution of* (3) *in compact form is given by:*

$$v = v_0 + v_1 + v_2 + \cdots . \tag{9}$$

4. Applications of the Problem

We provide some examples of the problems that are being discussed.

Example 1. *Examine* (3) *with the FF derivative provided as*

$$\begin{cases} {}^{FF}D^{\theta,\kappa}_{0,\ell} v(y,\ell) = -\left(3v^2 v_y + v_{yy} + \omega v_{yyy} + v_{yyyy}\right), \\ {}^{RL}D^{\theta-1}_{0,\ell} v(y,0) = y^2. \end{cases} \tag{10}$$

Using the previously described technique, we can apply the Laplace transform to write (10):

$$v(y,\ell) = \mathbb{L}^{-1}\{\frac{v_0}{s} + \frac{\kappa}{s^\theta}\mathbb{L}\{-t^{-1+\kappa}\{3v^2 v_y + v_{yy} + \omega v_{yyy} + v_{yyyy}\}\}\}. \tag{11}$$

With this condition ${}^{RL}D^{\theta-1}v(y,0) = y^2$, one may write from (11)

$$v(y,\ell) \quad = \quad \mathbb{L}^{-1}\{\frac{y^2}{s} + \frac{\kappa}{s^\theta}\mathbb{L}\{-t^{-1+\kappa}\{3v^2 v_y + v_{yy} + \omega v_{yyy} + v_{yyyy}\}\}\}. \tag{12}$$

Decomposing the nonlinear term $3v^2 v_y$ as follows:

$$v^2 v_y = \sum_{n=0}^{\infty} \mathbb{A}_n, \tag{13}$$

where $\mathbb{A}_n$ is given by

$$\mathbb{A}_n = \frac{1}{\Gamma(n+1)}\frac{d^n}{d\mu^n}\left[\left(\sum_{j=0}^{n}\mu^j v_j\right)^2 \sum_{j=0}^{n}\mu^j v_{j,y}\right]_{\mu=0}.$$

Certain terms are computed as

$$\begin{aligned}
\mathbb{A}_0 &= v_0^2 v_{0y}, \\
\mathbb{A}_1 &= 2v_0 v_1 v_{0y} + v_0^2 v_{1y}, \\
\mathbb{A}_2 &= v_1^2 v_{0y} + 2v_0 v_{0y} v_2 + v_0^2 v_{1y} + v_0 v_1 v_{1y} + 2v_0 v_{2y}.
\end{aligned}$$

Taking into account a solution in series form as

$$\sum_{n=0}^{\infty} v_n. \tag{14}$$

We find the solution by applying the same process as performed in the general algorithm, using (13) and (14) in (12):

$$\begin{aligned}
v_0(y,\ell) &= y^2, \\
v_1(y,\ell) &= -\frac{\kappa\Gamma(\kappa)\ell^{\theta+\kappa-1}}{\Gamma(\theta+\kappa-1)}(6y^5+2), \\
v_2(y,\ell) &= \frac{3\kappa\Gamma(\kappa)\Gamma(\theta+2\kappa-1)\ell^{2\theta+2\kappa-2}}{\Gamma(\theta+\kappa-1)\Gamma(2\theta+2\kappa-2)}(54y^8+128y^3+360y^2+720y), \\
v_3(y,t) &= \frac{90\kappa^2\Gamma(\kappa)\Gamma(\theta+2\kappa-1)\ell^{2\theta+2\kappa-2}}{\Gamma(\theta+\kappa-1)\Gamma(2\theta+2\kappa-2)}y^8 - \frac{9\kappa^2\Gamma(\kappa)\Gamma(\theta+2\kappa-1)\Gamma(2\theta+3\kappa-1)\ell^{3\theta+3\kappa-3}}{\Gamma(\theta+\kappa-1)\Gamma(2\theta+2\kappa-2)\Gamma(3\theta+3\kappa-3)} \\
&\quad (216y^{11}+512y^6+1440y^5+2880y^4) - \frac{\kappa^3(\Gamma(\kappa))^2\Gamma(2\theta+3\kappa-1)\ell^{3\theta+3\kappa-3}}{(\Gamma(\theta+\kappa-1))^2\Gamma(3\theta+3\kappa-3)} \\
&\quad (10872y^{11}+4848y^8+8y) - \frac{3\kappa^3\Gamma(\kappa)\Gamma(\theta+2\kappa-1)\Gamma(2\theta+3\kappa-1)\ell^{3\theta+3\kappa-3}}{\Gamma(\theta+\kappa-1)\Gamma(2\theta+2\kappa-2)\Gamma(3\theta+3\kappa-3)} \\
&\quad (2592y^7+3024\omega y^6+108864y^4+2304y^2+768\omega y+4320y+720\omega+5088).
\end{aligned}$$

and so forth. After a few terms, the solution appears as

$$\begin{aligned}
\mathrm{v}(y,\ell) &= y^2 - \frac{\kappa\Gamma(\kappa)\ell^{\theta+\kappa-1}}{\Gamma(\theta+\kappa-1)}(6y^5+2) + \frac{3\kappa\Gamma(\kappa)\Gamma(\theta+2\kappa-1)^{2\theta+2\kappa-2}}{\Gamma(\theta+\kappa-1)\Gamma(2\theta+2\kappa-2)} \\
&\quad (54y^8+128y^3+360y^2+720y) - \frac{90\kappa^2\Gamma(\kappa)\Gamma(\theta+2\kappa-1)\ell^{2\theta+2\kappa-2}}{\Gamma(\theta+\kappa-1)\Gamma(2\theta+2\kappa-2)}y^8 \\
&- \frac{9\kappa^2\Gamma(\kappa)\Gamma(\theta+2\kappa-1)\Gamma(2\theta+3\kappa-1)\ell^{3\theta+3\kappa-3}}{\Gamma(\theta+\kappa-1)\Gamma(2\theta+2\kappa-2)\Gamma(3\theta+3\kappa-3)} \\
&\quad (216y^{11}+512y^6+1440y^5+2880y^4) - \frac{\kappa^3(\Gamma(\kappa))^2\Gamma(2\theta+3\kappa-1)\ell^{3\theta+3\kappa-3}}{(\Gamma(\theta+\kappa-1))^2\Gamma(3\theta+3\kappa-3)}(10872y^{11} \\
&\quad +4848y^8+8y) - \frac{3\kappa^3\Gamma(\kappa)\Gamma(\theta+2\kappa-1)\Gamma(2\theta+3\kappa-1)\ell^{3\theta+3\kappa-3}}{\Gamma(\theta+\kappa-1)\Gamma(2\theta+2\kappa-2)\Gamma(3\theta+3\kappa-3)} \\
&\quad (2592y^7+3024\omega y^6+108864y^4+2304y^2+768\omega y+4320y \\
&+ 720\omega+5088)+\cdots.
\end{aligned} \tag{15}$$

Plot the of the preceding series solution of (15) is given in Figure-1, for different values of θ, κ and for fixed value of $\omega = 1$.

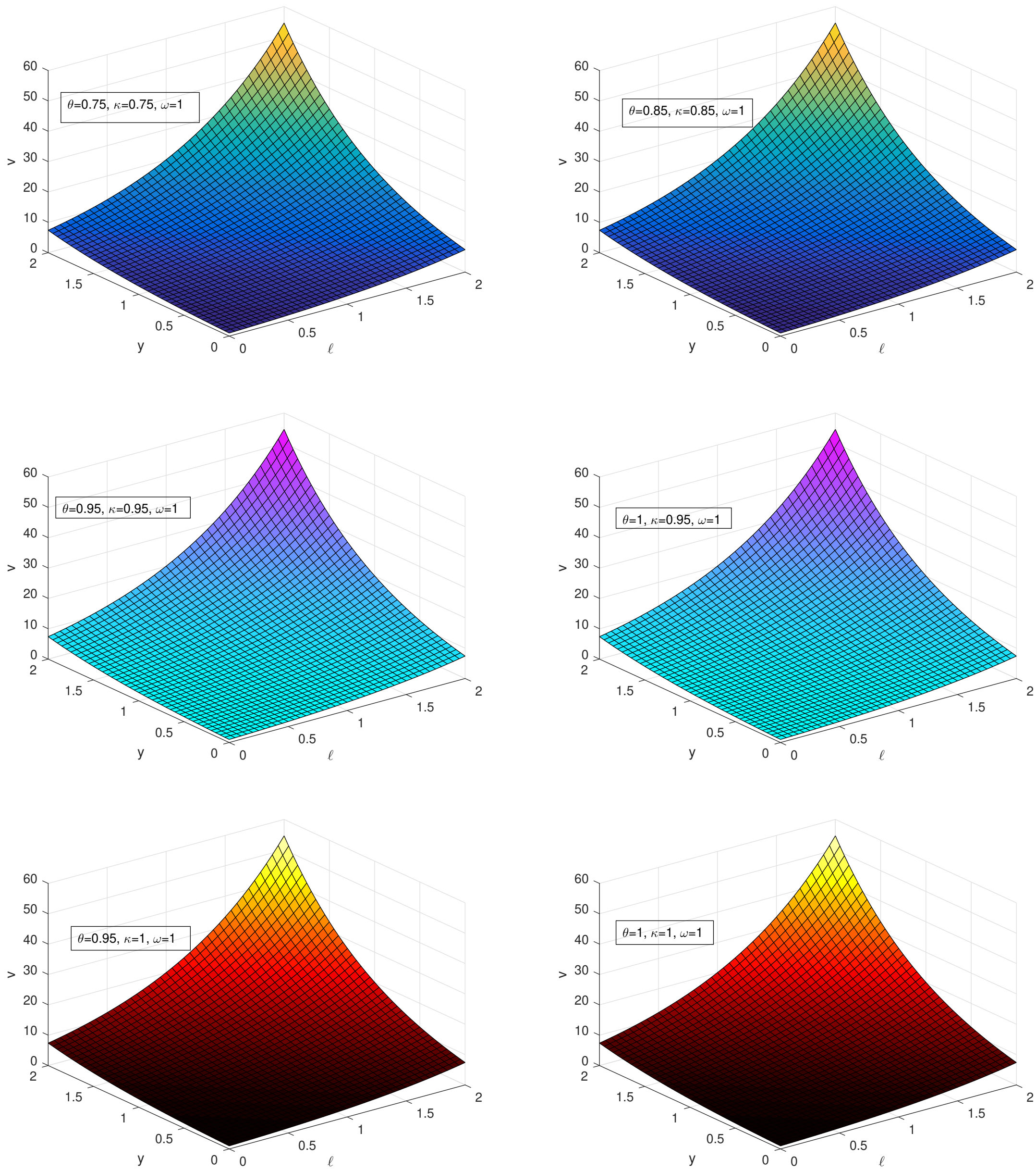

Figure 1: Visual exploration of v for different values of θ, κ and for fixed value of ω.

Example 2. *Consider the following problem using* (3)*:*

$$\begin{aligned} &{}^{FF}D^{\theta,\kappa}_{0,\ell}v(y,\ell) = -\left(3v^2v_y + v_{yy} + \omega v_{yyy} + v_{yyyy}\right), \\ &{}^{RL}D^{\theta-1}v(y,0) = \cos y. \end{aligned} \tag{16}$$

Using the previously described technique, we can apply the Laplace transform to write (16):

$$v(y,\ell) = \mathbb{L}^{-1}\{\frac{v_0}{s} + \frac{\kappa}{s^\theta}\mathbb{L}\{-t^{-1+\kappa}\{3v^2v_y + v_{yy} + \omega v_{yyy} + v_{yyyy}\}\}\}. \tag{17}$$

With v$(y,0) = \cos y$, one may write from (17) as

$$v(y,\ell) = \mathbb{L}^{-1}\{\frac{\cos y}{s} + \frac{\kappa}{s^\theta}\mathbb{L}\{-t^{-1+\kappa}\{3v^2v_y + v_{yy} + \omega v_{yyy} + v_{yyyy}\}\}\}. \tag{18}$$

The nonlinear expression $3v^2(y,t)v_y(y,t)$ can be broken down as follows:

$$v^2(y,t)v_y(y,t) = \sum_{n=0}^{\infty} \mathbb{A}_n, \tag{19}$$

where $\mathbb{A}_n$ is given by

$$\mathbb{A}_n = \frac{1}{\Gamma(n+1)}\frac{d^n}{d\mu^n}\left[\left(\sum_{j=0}^{n}\mu^j v_j(y,t)\right)^2 \sum_{j=0}^{n}\mu^j v_{j,y}(y,t)\right]_{\mu=0}. \tag{20}$$

Calculating few terms as given as:

$$\begin{aligned} \mathbb{A}_0 &= v_0^2 v_{0y}, \\ \mathbb{A}_1 &= 2v_0v_1v_{0y} + v_0^2v_{1y}, \\ \mathbb{A}_2 &= v_1^2v_{0y} + 2v_0v_{0y}v_2 + v_0^2v_{1y} + v_0v_1v_{1y} + 2v_0v_{2y}. \end{aligned}$$

Taking into account the solution in a series form as:

$$\sum_{n=0}^{\infty} v_n. \tag{21}$$

We find the solution by applying the same process as performed in the general algorithm, using (19) and (21) in (18):

$$\begin{aligned} v_0(y,\ell) &= \cos y, \\ v_1(y,\ell) &= -\frac{\kappa\Gamma(\kappa)\ell^{\theta+\kappa-1}}{\Gamma(\theta+\kappa-1)}(-3\cos^2 y\sin y + \omega\sin y), \\ v_2(y,\ell) &= \frac{\kappa^2\Gamma(\kappa)\Gamma(\theta+2\kappa-1)\ell^{2\theta+2\kappa-2}}{\Gamma(\theta+\kappa-1)\Gamma(2\theta+2\kappa-2)}(36\cos^3 y\sin^2 y - 6\omega\cos y\sin^2 y - 9\cos^5 y + 3\omega\cos^3 y \\ &\quad +54\sin^3 y + 21\cos^2 y\sin y + 60\omega\sin^3 y - 183\omega\cos^2 y\sin y + \omega^2\sin y - 183\cos^2 y\sin y), \end{aligned}$$

$$
\begin{aligned}
v_3(y,\ell) &= \frac{3\kappa^2\Gamma(\kappa)\Gamma(\theta+2\kappa-1)\ell^{2\theta+2\kappa-2}}{\Gamma(\theta+\kappa-1)}(-3\cos^4 y\sin y+\omega\cos^2 y\sin y) \\
&\quad -\frac{3\kappa^2(\Gamma(\kappa))^2\Gamma(2\theta+3\kappa-2)\ell^{3\theta+3\kappa-3}}{\Gamma(\theta+\kappa-1)\Gamma(2\theta+2\kappa-2)\Gamma(3\theta+3\kappa-3)}(-27\cos^4 y\sin^3 y-\beta^2\sin^3 y \\
&\quad +12\beta^2\cos^2 y\sin^3 y+9\cos^6 y\sin y-3\beta\cos^4 y\sin y+\beta^2\cos^2 y\sin y) \\
&\quad +\frac{3\kappa^2\Gamma(\kappa)\Gamma(\theta+2\kappa-1)\Gamma(2\theta+3\kappa-2)\ell^{3\theta+3\kappa-3}}{\Gamma(\theta+\kappa-1)\Gamma(2\theta+2\kappa-2)\Gamma(3\theta+3\kappa-3)} \\
&\quad (-216\cos^y 3\sin^3 y+324\cos^5 y\sin y+12\omega\cos y\sin^3 y-42\omega\cos^3 y\sin y \\
&+ 772\cos^2 y\sin^2 y-324\cos^4 y+360\cos y\sin^2 y-366\omega\cos^4 y+532\omega\cos^2 y\sin^2 y \\
&+ 2\omega^2\sin^2 y+72\cos^4 y\sin^3 y-12\omega\cos^2 y\sin^3 y-18\cos^6 y\sin y+6\omega\cos^4 y\sin y \\
&+ 108\cos y\sin^4 y+42\cos^3 y\sin^2 y+120\omega\cos y\sin^4 y-366\omega\cos^3 y\sin^2 y+2\omega^2\cos y\sin^2 y \\
&- 1058\cos^3 y\sin^2 y+216\cos y\sin^4 y+117\cos^5 y+60\omega\cos y\sin^2 y-21\omega\cos^3 y \\
&+ 1258\cos^2 y\sin y-652\sin^3 y+360\omega\cos y\sin y+1081\cos^2 y\sin y-\omega^2\sin y-216\omega\sin^5 y \\
&+ 3240\omega\cos^2 y\sin^3 y-2169\omega\cos^4 y\sin y+99\omega^2\cos^2 y\sin y-60\omega^2\sin^3 y \\
&+ 84\omega^2\cos^3 y\sin y-3674\omega\cos y\sin^2 y+1258\omega\cos^3 y+360\omega^2\cos^2 y-360\omega^2\sin^2 y \\
&+ 1081\omega^2\sin^3 y-2960\omega^2\cos y\sin^2 y-\omega^3\cos y-7560\cos y\sin^4 y \\
&+ 18396\cos^3 y\sin^2 y-2169\cos^5 y-99\omega\cos^3 y-198\omega\cos y\sin^2 y-180\omega\sin^2 y \\
&- 252\omega\cos^2 y\sin^2 y+84\beta\cos^4 y-7348\cos^2 y\sin^2 y-3674\sin^3 y-1440\omega\cos y\sin y \\
&- 9163\omega\cos^2 y\sin y+2960\omega\sin^3 y+\omega^2\sin y).
\end{aligned}
$$

Therefore, the solution may be written as

$$
\begin{aligned}
v(y,\ell) &= \cos y-\frac{\kappa\Gamma(\kappa)\ell^{\theta+\kappa-1}}{\Gamma(\theta+\kappa-1)}(-3\cos^2 y\sin y+\omega\sin y)+\frac{\kappa^2\Gamma(\kappa)\Gamma(\theta+2\kappa-1)\ell^{2\theta+2\kappa-2}}{\Gamma(\theta+\kappa-1)\Gamma(2\theta+2\kappa-2)} \\
&\quad (36\cos^3 y\sin^2 y-6\omega\cos y\sin^2 y-9\cos^5 y+3\omega\cos^3 y+54\sin^3 y+21\cos^2 y\sin y \\
&+ 60\omega\sin^3 y-183\omega\cos^2 y\sin y+\omega^2\sin y-183\cos^2 y\sin y) \\
&\quad +\frac{3\kappa^2\Gamma(\kappa)\Gamma(\theta+2\kappa-1)\ell^{2\theta+2\kappa-2}}{\Gamma(\theta+\kappa-1)}(-3\cos^4 y\sin y+\omega\cos^2 y\sin y) \\
&\quad -\frac{3\kappa^2(\Gamma(\kappa))^2\Gamma(2\theta+3\kappa-2)\ell^{3\theta+3\kappa-3}}{\Gamma(\theta+\kappa-1)\Gamma(2\theta+2\kappa-2)\Gamma(3\theta+3\kappa-3)}(-27\cos^4 y\sin^3 y-\beta^2\sin^3 y \\
&\quad +12\beta^2\cos^2 y\sin^3 y+9\cos^6 y\sin y-3\beta\cos^4 y\sin y+\beta^2\cos^2 y\sin y) \\
&\quad +\frac{3\kappa^2\Gamma(\kappa)\Gamma(\theta+2\kappa-1)\Gamma(2\theta+3\kappa-2)\ell^{3\theta+3\kappa-3}}{\Gamma(\theta+\kappa-1)\Gamma(2\theta+2\kappa-2)\Gamma(3\theta+3\kappa-3)}(-216\cos^3 y\sin^3 y \\
&\quad +324\cos^5 y\sin y+12\omega\cos y\sin^3 y-42\omega\cos^3 y\sin y+772\cos^2 y\sin^2 y \\
&\quad -324\cos^4 y+360\cos y\sin^2 y-366\omega\cos^4 y+532\omega\cos^2 y\sin^2 y+2\omega^2\sin^2 y \\
&\quad +72\cos^4 y\sin^3 y-12\omega\cos^2 y\sin^3 y-18\cos^6 y\sin y+6\omega\cos^4 y\sin y \\
&\quad +108\cos y\sin^4 y+42\cos^3 y\sin^2 y+120\omega\cos y\sin^4 y-366\omega\cos^3 y\sin^2 y \\
&\quad +2\omega^2\cos y\sin^2 y-1058\cos^3 y\sin^2 y+216\cos y\sin^4 y+117\cos^5 y+60\omega\cos y\sin^2 y
\end{aligned}
$$

$$
\begin{aligned}
&- \quad 21\omega\cos^3 y + 1258\cos^2 y\sin y - 652\sin^3 y + 360\omega\cos y\sin y + 1081\cos^2 y\sin y \\
&- \quad \omega^2\sin y - 216\omega\sin^5 y + 3240\omega\cos^2 y\sin^3 y - 2169\omega\cos^4 y\sin y + 99\omega^2\cos^2 y\sin y \\
&\quad\; -60\omega^2\sin^3 y + 84\omega^2\cos^3 y\sin y - 3674\omega\cos y\sin^2 y + 1258\omega\cos^3 y + 360\omega^2\cos^2 y \\
&- \quad 360\omega^2\sin^2 y + 1081\omega^2\sin^3 y - 2960\omega^2\cos y\sin^2 y - \omega^3\cos y - 7560\cos y\sin^4 y \\
&\quad\; +18396\cos^3 y\sin^2 y - 2169\cos^5 y - 99\omega\cos^3 y - 198\omega\cos y\sin^2 y - 180\omega\sin^2 y \\
&- \quad 252\omega\cos^2 y\sin^2 y + 84\beta\cos^4 y - 7348\cos^2 y\sin^2 y - 3674\sin^3 y - 1440\omega\cos y\sin y \\
&- \quad 9163\omega\cos^2 y\sin y + 2960\omega\sin^3 y + \omega^2\sin y) + \cdots . \qquad (22)
\end{aligned}
$$

A plot of the previous solution of (22) is given in Figure 2 for different values of θ, κ and for a fixed value of $\omega = 1$.

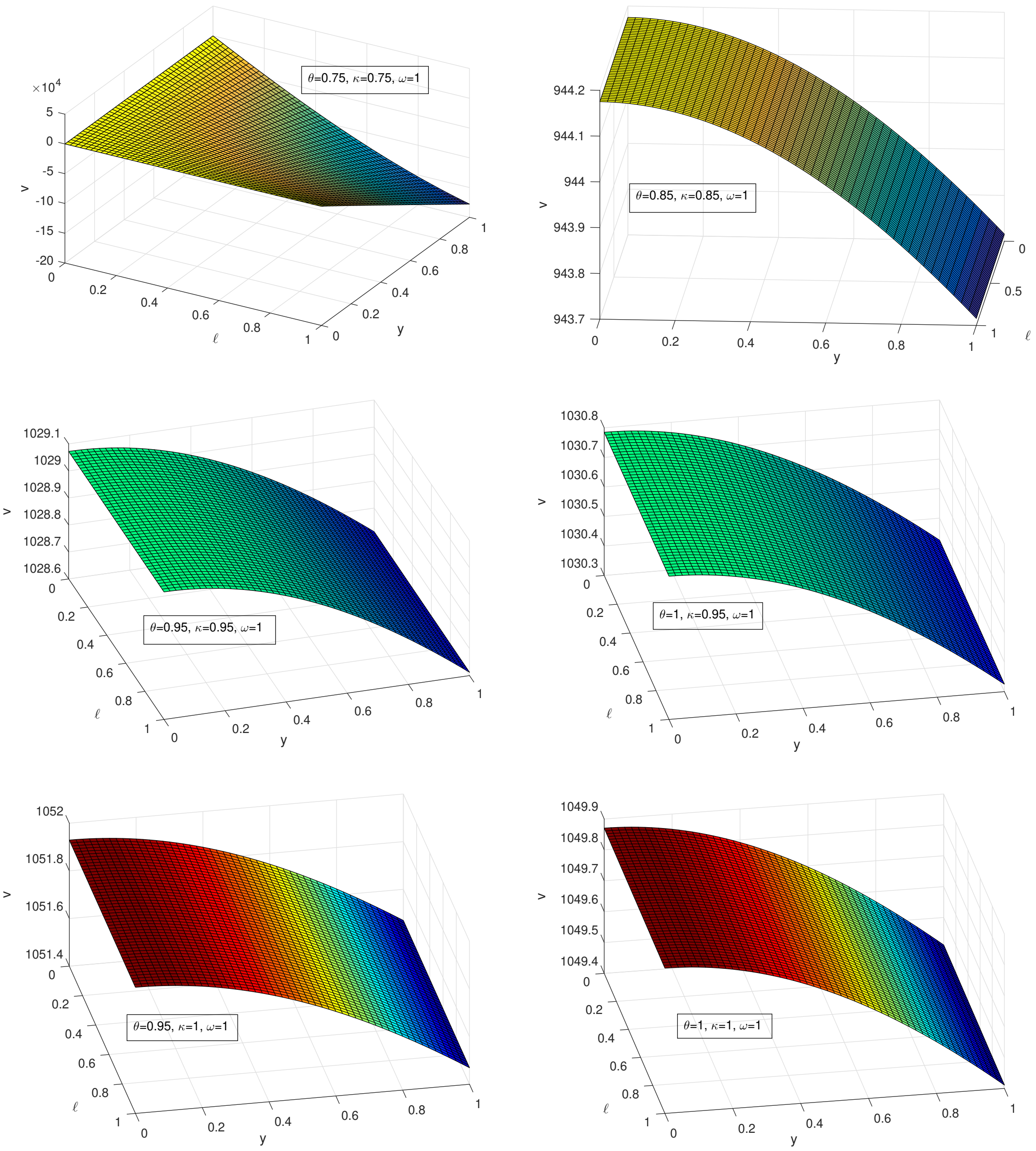

Figure 2: Visual exploration of v for different values of θ, κ and for fixed value of $\omega = 1.0$.

Both Figure 1 and Figure 2 show that as the fractional and fractal values approach 1, the solution curves approach the classical solution curves. Clearly one can see the impact of fractal and fractional orders on the dynamics of the specified problem.

5. Neural Network Validation

To enhance the analysis, we consider three distinct cases in this example. To evaluate the accuracy of the proposed approach, a NN based on the LM algorithm is employed, supported by regression analysis and error distribution statistics. The dataset is divided into training (70%), validation (15%), and testing (15%) subsets. The network input consists of spatiotemporal pairs (v, ℓ), while the output corresponds to the predicted value $\psi(v, \ell)$. The hidden layer employs the `tansig` activation function, while the output layer is linear.

Case 1: In this case, for the simulation's purpose, we used the same solution and data as the current example.

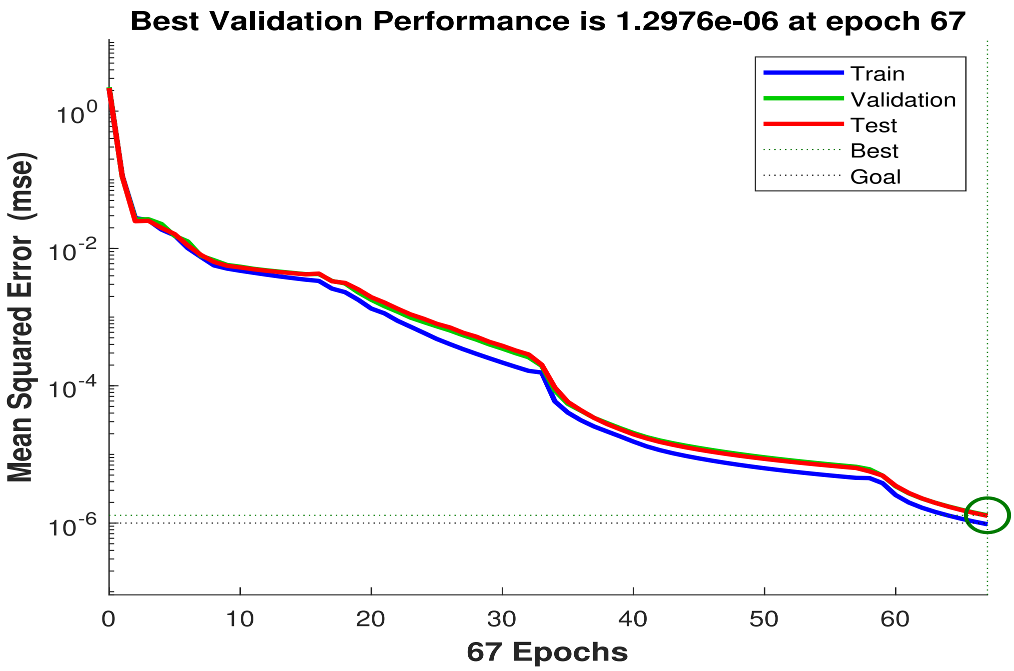

Figure 3: MSE performance of the model at epoch 67.

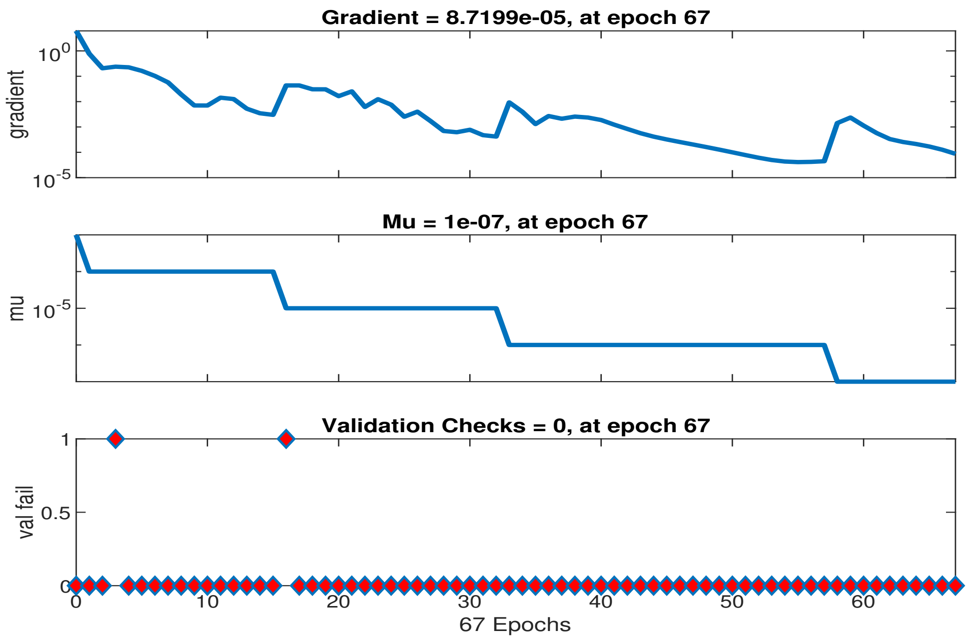

Figure 4: Training test of the model at epoch 67.

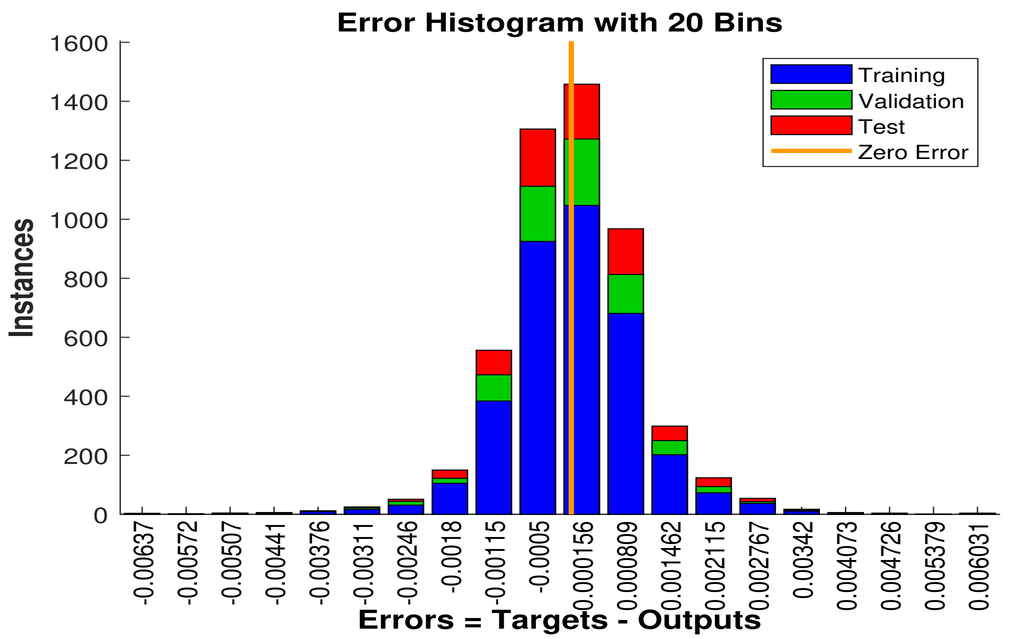

Figure 5: Training histogram of the model at epoch 67.

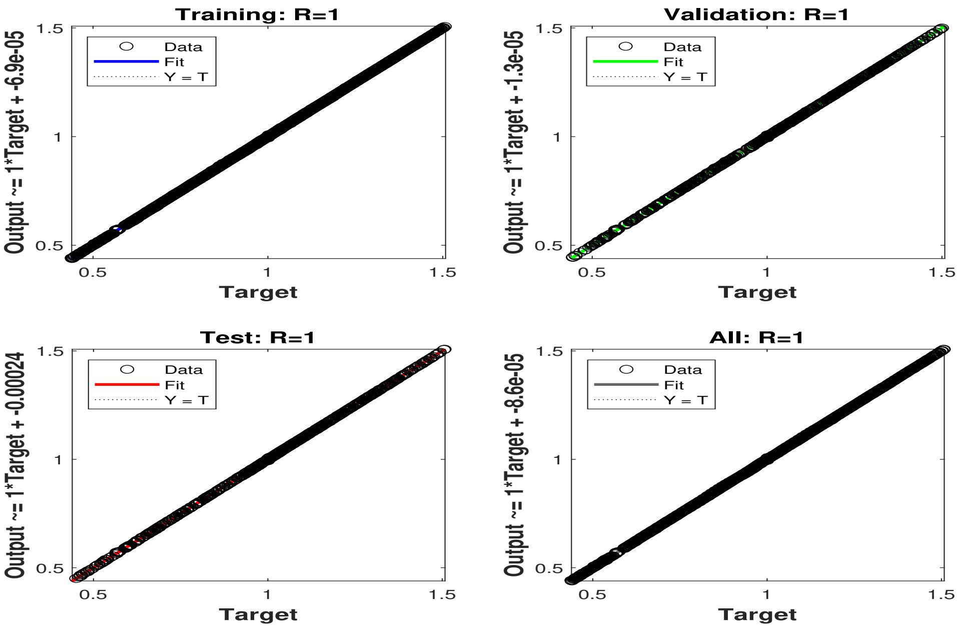

Figure 6: Training regression of the model at epoch 67.

Figures 3-6 provide illustrations of MSE performance and training tests of the model (3) for $\theta = 0.95$, $\kappa = 1$ and $\omega = 1$.

Case 2: In the current case, we use the same information as in the preceding case; the only difference lies in the values of θ and κ.

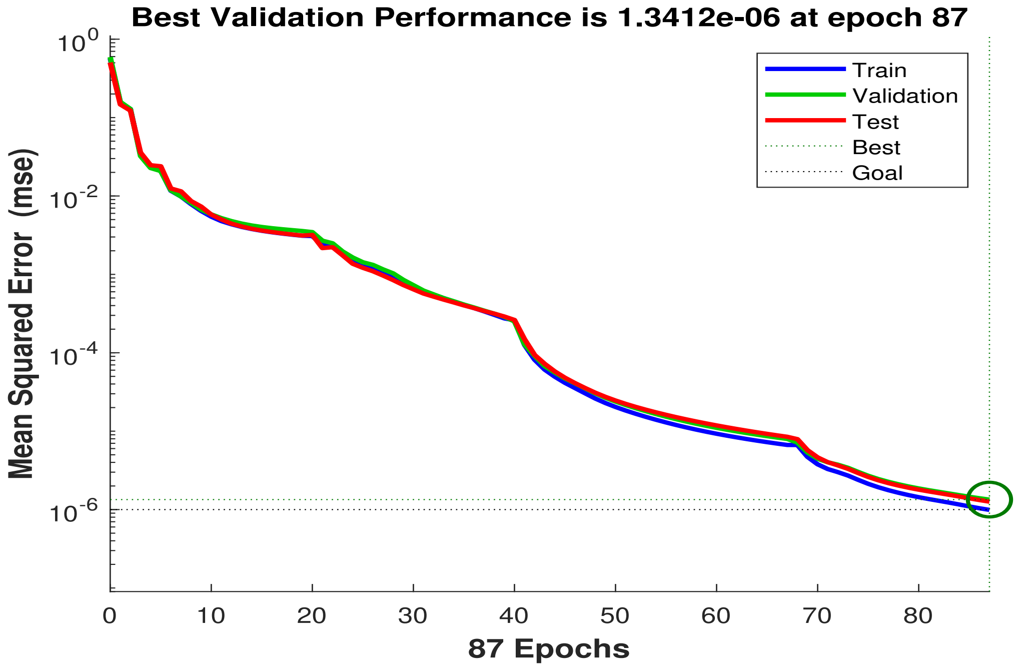

Figure 7: MSE performance of the model at epoch 87.

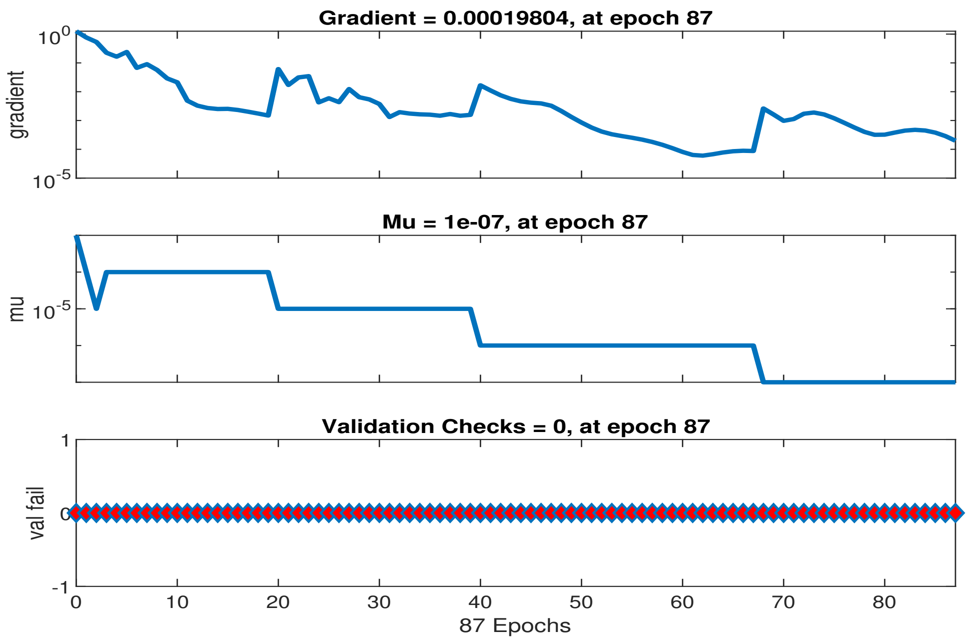

Figure 8: Training test of the model at epoch 87.

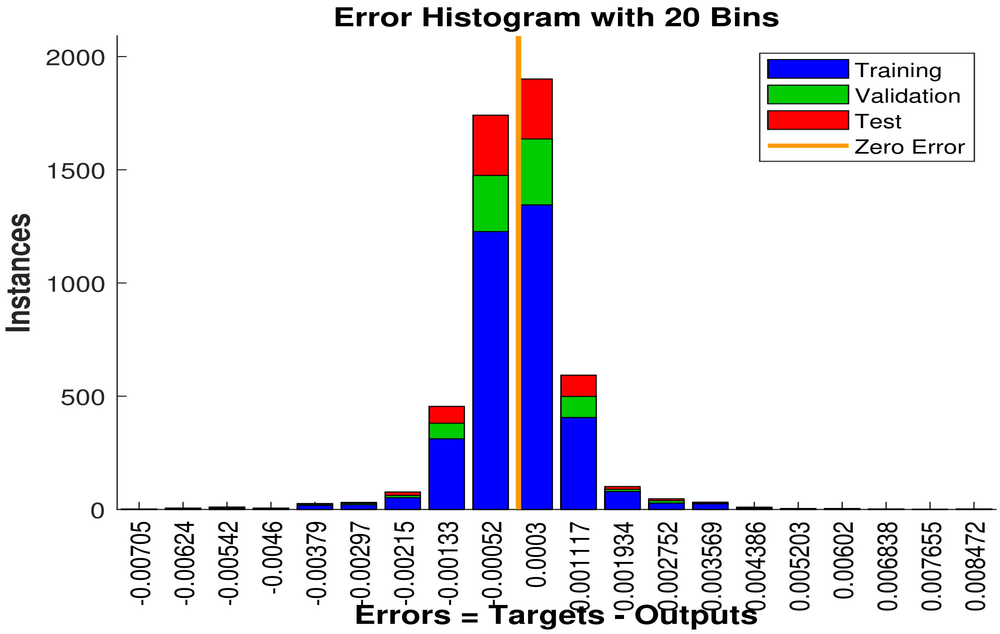

Figure 9: Training histogram of the model at epoch 87.

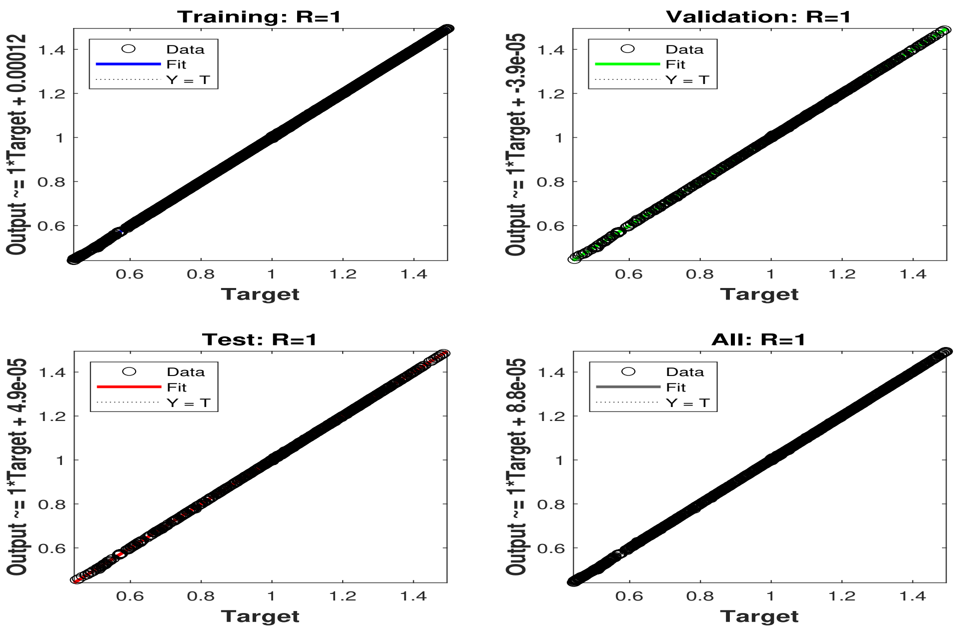

Figure 10: Training regression of the model at epoch 87.

Figures 7-10 provide illustrations of MSE performance and training tests of the model (3) for $\theta = 1$, $\kappa = 0.95$ and $\omega = 1$.

Case 3: To study more about the ongoing analysis, we consider one more case for different θ and κ values.

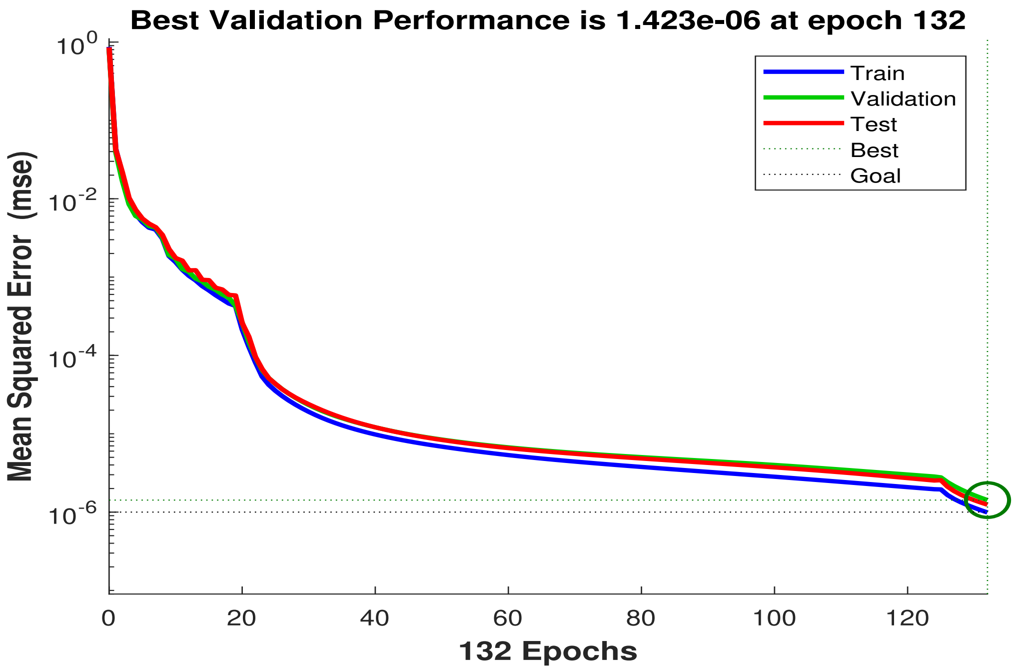

Figure 11: MSE performance of the model at epoch 132.

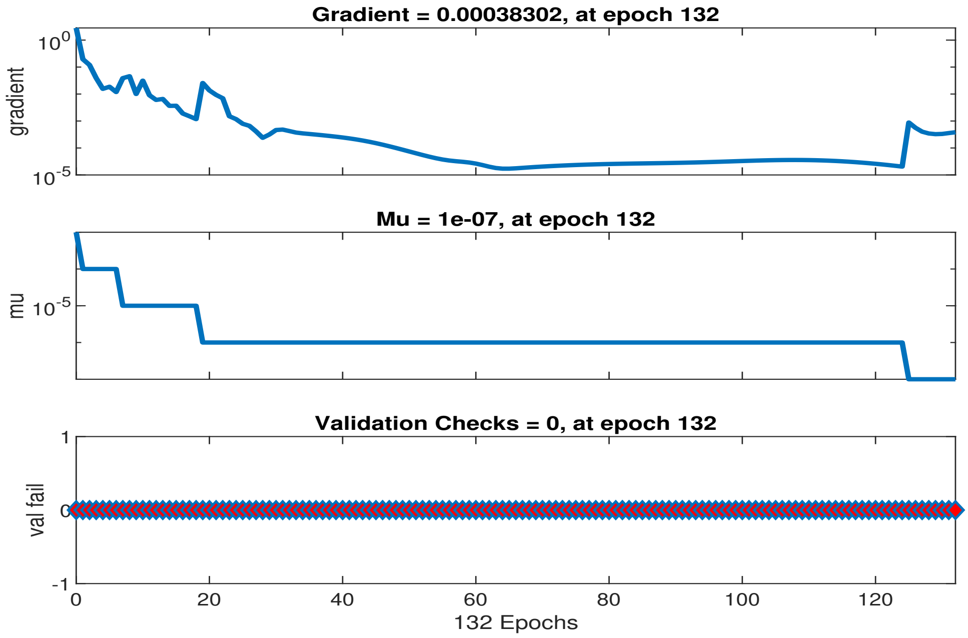

Figure 12: Training test of the model at epoch 132.

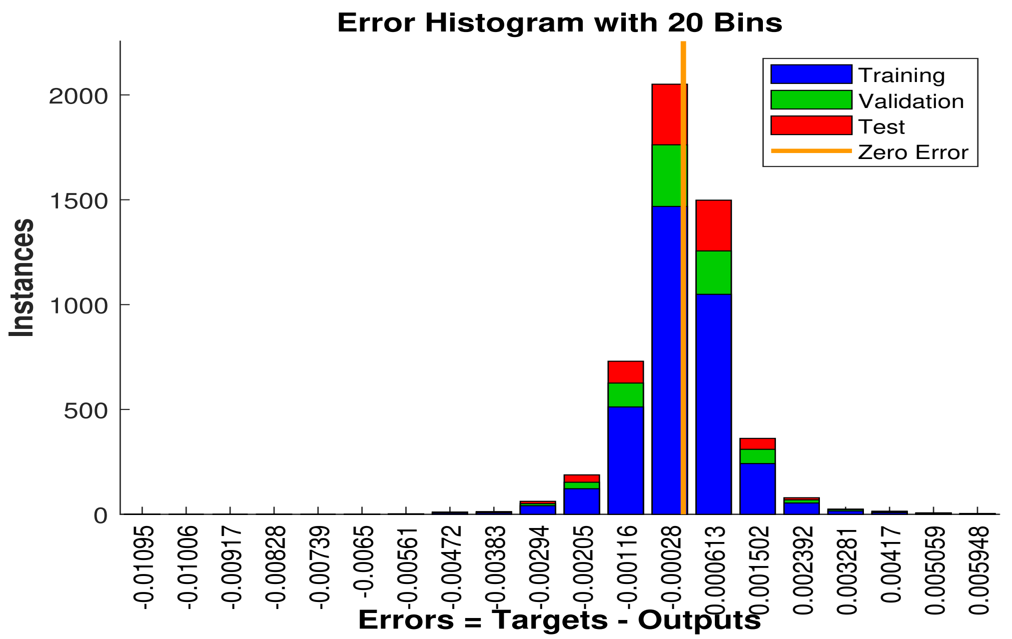

Figure 13: Training histogram of the model at epoch 132.

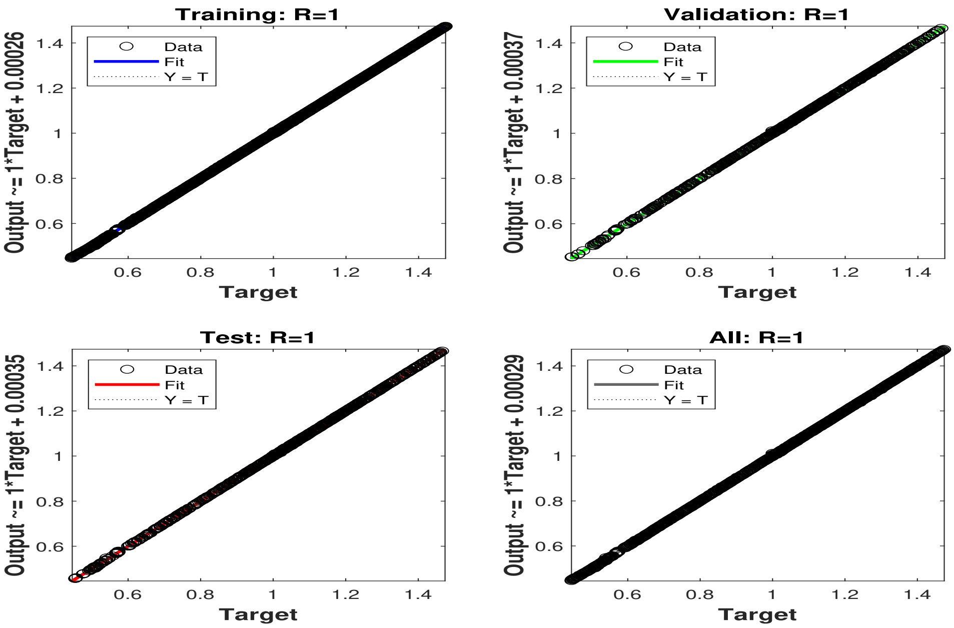

Figure 14: Training regression of the model at epoch 132.

Figures 11-14 show illustrations of MSE performance and training tests of the model (3) for $\theta = 0.95$, $\kappa = 0.95$ and $\omega = 1$.

It is clear from the above three cases that the influence of fractional order θ and fractal order κ on the NN convergence rate. When $\theta = 1$ and $\kappa = 0.95$, the network converges in approximately 67 epochs, reflecting a relatively smooth and near-classical dynamic behaviour. For $\theta = 0.95$ and $\kappa = 1$, the number of epochs rises to 87, indicating that fractional memory effects introduce additional complexity in the learning process.The most computationally demanding case corresponds to $\theta = 0.95$ and $\kappa = 0.95$, where convergence requires 132 epochs. This slower convergence can be attributed to the combined influence of fractional memory and fractal heterogeneity, which increase the nonlinearity of the system and the richness of its dynamic patterns.

Table 1: NN performance metrics for the FF BE.

Case	θ	κ	MSE	R	Epochs / Time (s)	ω
1	0.95	1.0	1.297×10^{-6}	1.0	67 / 4.12	1.0
2	1.0	0.95	1.3412×10^{-6}	1.0	87 / 4.85	1.0
3	0.95	0.95	1.423×10^{-6}	1.0	132 / 5.10	1.0

Table 1 summarizes the performance of the NN validation for the FF BE solved through the LADM. The results correspond to different values of θ and κ.

5.1. Quantitative Comparison Between NN and LADM Solutions

A quantitative comparison between the NN predictions and the analytical solutions obtained by the LADM has been carried out. The Mean Absolute Error (MAE) and Root Mean Square Error (RMSE) are calculated for several combinations of the fractional order θ and the fractal order κ. Lower MAE and RMSE values reflect a strong agreement between both approaches, indicating that the trained NN successfully captures the complex FF dynamics embedded within the BE.

Table 2: Comparison between NN predictions and LADM solutions for different values of θ and κ.

Case	$\boldsymbol{\theta}$	$\boldsymbol{\kappa}$	**MAE**	**RMSE**
1	0.25	0.60	1.87×10^{-3}	2.41×10^{-3}
2	0.40	0.70	1.35×10^{-3}	1.78×10^{-3}
3	0.55	0.80	1.02×10^{-3}	1.43×10^{-3}
4	0.70	0.90	8.40×10^{-4}	1.09×10^{-3}
5	1.00	1.00	6.92×10^{-4}	8.85×10^{-4}

It can be clearly observed from Table 2 that the MAE and RMSE values decrease as θ and κ increase, implying improved smoothness and reduced deviation between NN and LADM solutions.

6. Conclusion

In the manuscript, nonlinear BE under FF derivative has been investigated. We have used LADM to obtain the approximate series solutions; the validity of the solutions was confirmed via NN-based validation. The findings illustrate the effectiveness of the FF Benney model in describing nonlinear dispersive wave dynamics with memory and self-similarity effects. The hybrid framework suggested in our study properly integrates analytical and computational methods to provide promising approaches for modelling problems in fluid dynamics, nonlinear optics, and signal processing. Future research can be extended to other nonlocal fractional operators and investigate the possibility of deep learning integration to further improve computational performance and accuracy.

Declaration of competing interest

The authors declare no financial or personal conflicts of interest affecting this work.

Funding

No funding source exists.

Acknowledgements

The authors would like to thank Prince Sultan University for paying the APC and for the support through the TAS research lab.

Data Availability

All data is included in the paper.

References

[1] T. Abdeljawad, N. Khan, B. Abdalla, A. A. Jaser, M. Alqudah, and K. Shah. A mathematical analysis of human papilloma virus (hpv) disease with new perspectives of fractional calculus. *Alexandria Engineering Journal*, 125:575–599, 2025.

[2] M. Khan, I. Ullah, N. Khan, S. Hussain, and M. I. L. Khattak. Adpnet: Attention-driven dual-path network for automated polyp segmentation in colonoscopy. *Image and Vision Computing*, page 105648, 2025.

[3] K. Shah, I. Ahmad, and T. Abdeljawad. On non-linear fractional order coupled pantograph differential equations under nonlocal boundary conditions. *TWMS Journal of Applied and Engineering Mathematics*, 15(1):65–78, 2024.

[4] N. Khan, A. Ali, A. Ullah, and Z. A. Khan. Mathematical analysis of neurological disorder under fractional order derivative. *AIMS Mathematics*, 8(8):18846–18865, 2023.

[5] M. Khan, N. Khan, I. Ullah, K. Shah, T. Abdeljawad, and B. Abdalla. A novel fractal fractional mathematical model for hiv/aids transmission stability and sensitivity with numerical analysis. *Scientific Reports*, 15(1):9291, 2025.

[6] S. M. A. Shah, Y. Nie, A. Alkhazzan, C. Tunç, and A. Din. A stochastic hepatitis b model with media coverage and lévy noise. *Journal of Taibah University for Science*, 18(1):2414523, 2024.

[7] S. M. A. Shah, Y. Nie, A. Din, and A. Alkhazzan. Stochastic optimal control analysis for hbv epidemic model with vaccination. *Journal of Applied Mathematical Modelling and Simulation*, 2024.

[8] S. M. A. Shah, Y. Nie, A. Din, and A. Alkhazzan. Dynamics of hepatitis b virus transmission with a lévy process and vaccination effects. *Mathematics*, 12(11):1645, 2024.

[9] S. M. A. Shah, H. Tahir, A. Khan, W. A. Khan, and A. Arshad. Stochastic model on the transmission of worms in wireless sensor network. *Journal of Mathematical Techniques in Modeling*, 1(1), 2024.

[10] S. M. A. Shah, Y. Nie, A. Din, A. Alkhazzan, and B. Younas. Stochastic modeling and analysis of hepatitis and tuberculosis co-infection dynamics. *Chinese Physics B*, 33(11):110203, 2024.

[11] A. Alkhazzan, J. Wang, Y. Nie, S. M. A. Shah, D. K. Almutairi, H. Khan, and

J. Alzabut. Lyapunov-based analysis and worm extinction in wireless networks using stochastic sveir model. *Alexandria Engineering Journal*, 118:337–353, 2025.

[12] S. M. A. Shah, Y. Nie, A. Din, A. Alkhazzan, A. Arshad, and B. Younas. Stochastic modeling for the transmission of hepatitis b virus with multiple time-delays and vaccination effect. *Arabian Journal of Mathematics*, pages 1–30, 2025.

[13] R. Hilfer. *Applications of Fractional Calculus in Physics.* World Scientific, Singapore, 2000.

[14] A. A. Kilbas, H. M. Srivastava, and J. J. Trujillo. *Theory and Applications of Fractional Differential Equations.* Elsevier, Amsterdam, 2006.

[15] A. Atangana. Fractal-fractional differentiation and integration: connecting fractal calculus and fractional calculus to predict complex system. *Chaos, Solitons & Fractals*, 102:396–406, 2017.

[16] P. Li, L. Han, C. Xu, X. Peng, M. U. Rahman, and S. Shi. Dynamical properties of a meminductor chaotic system with fractal–fractional power law operator. *Chaos, Solitons & Fractals*, 175:114040, 2023.

[17] K. A. Abro and A. Atangana. Mathematical analysis of memristor through fractal-fractional differential operators: a numerical study. *Mathematical Methods in the Applied Sciences*, 43(10):6378–6395, 2020.

[18] K. Ahmed, H. Adam, M. Y. Youssif, and S. Saber. Different strategies for diabetes by mathematical modeling: Applications of fractal–fractional derivatives in the sense of atangana–baleanu. *Results in Physics*, 52:106892, 2023.

[19] M. U. Rahman, M. Arfan, Z. Shah, and E. Alzahrani. Evolution of fractional mathematical model for drinking under atangana-baleanu caputo derivatives. *Physica Scripta*, 96(11):115203, 2021.

[20] J. F. Gomez-Aguilar, T. Cordova-Fraga, T. Abdeljawad, A. Khan, and H. Khan. Analysis of fractal–fractional malaria transmission model. *Fractals*, 28(8):2040041, 2020.

[21] M. A. Khan, A. Cicik, and A. Ebraheem. Correction to: Analysis of dengue model with fractal-fractional caputo–fabrizio operator. *Advances in Difference Equations*, 2021(1), 2021.

[22] A. Atangana and S. Qureshi. Modeling attractors of chaotic dynamical systems with fractal–fractional operators. *Chaos, Solitons & Fractals*, 123:320–337, 2019.

[23] K. A. Abro. Role of fractal–fractional derivative on ferromagnetic fluid via fractal laplace transform: A first problem via fractal–fractional differential operator. *European Journal of Mechanics-B/Fluids*, 85:76–81, 2021.

[24] K. Shah, I. Ahmad, Shafiullah, A. Mukheimer, T. Abdeljawad, and M. B. Jeelani. On the existence and numerical simulation of cholera epidemic model. *Open Physics*, 2024.

[25] I. Ahmad, N. Ahmad, K. Shah, and T. Abdeljawad. Some appropriate results for the existence theory and numerical solutions of fractals–fractional order malaria disease mathematical model. *Results in Control and Optimization*, 14:100386, 2024.

[26] D. Proment and M. Onorato. A note on an alternative derivation of the benney equations for short wave-long wave interactions. *European Journal of Mechanics-*

B/Fluids, 34:1–6, 2012.

[27] R. Shah, Y. Alkhezi, and K. Alhamad. An analytical approach to solve the fractional benney equation using the q-homotopy analysis transform method. *Symmetry*, 15(3), 2023.

[28] M. A. Akinlar, A. Secer, and M. Bayram. Numerical solution of fractional benney equation. *Applied Mathematics and Information Sciences*, 8(4):1633–1637, 2014.

[29] H. Konno and P. S. Lomdahl. The birth-death stochastic processes of solitons in the 1d benney equation. *Journal of the Physical Society of Japan*, 69:1629–1641, 2000.

[30] K. Shah and T. Abdeljawad. On complex fractal-fractional order mathematical modeling of co2 emanations from energy sector. *Physica Scripta*, 99(1):015226, 2023.

[31] L. Zhang, M. U. Rahman, S. Ahmad, M. B. Riaz, and F. Jarad. Dynamics of fractional order delay model of coronavirus disease. *AIMS Mathematics*, 7(3):4211–4232, 2022.

[32] Waseem, S. Ali, and M. U. Rahman. Analysis of ebola virus model using intelligent computing of a new stochastic neural network. *International Journal of Biomathematics*, page 2450162, 2025.

[33] S. Tabassum and M. U. Rahman. Exploring corruption dynamics through caputo fractional models with deep neural network interventions. *Journal of Applied Mathematics and Computing*, 71(2):2703–2726, 2025.

[34] Eiman, K. Shah, M. Sarwar, T. Abdeljawad, and B. Abdalla. Analytical study of fractals fractional order (3 + 1) dimensional population dynamical model. *Fractals*, 2025.